



Original research

## The shikimate pathway regulates programmed cell death

Xuerui Lu<sup>a, b</sup>, Shixi Shi<sup>a, b</sup>, Chong Wu<sup>a, b</sup>, Xueao Zheng<sup>a, b</sup>, Chenkun Yang<sup>b, c</sup>, Jie Luo<sup>b, c</sup>,  
Shunping Yan<sup>a, b, \*</sup>

<sup>a</sup> Hubei Hongshan Laboratory, Wuhan, Hubei 430070, China

<sup>b</sup> College of Life Science and Technology, Huazhong Agricultural University, Wuhan, Hubei 430070, China

<sup>c</sup> National Key Laboratory of Crop Genetic Improvement, Huazhong Agricultural University, Wuhan, Hubei 430070, China



### ARTICLE INFO

#### Article history:

Received 24 January 2022

Received in revised form

28 January 2022

Accepted 2 February 2022

Available online 12 February 2022

#### Keywords:

Programmed cell death

Shikimate pathway

Lesion-mimic mutant

Immunity

Photoperiod

Arabidopsis

### ABSTRACT

Programmed cell death (PCD) is essential for both plant development and stress responses including immunity. However, how plants control PCD is not well-understood. The shikimate pathway is one of the most important metabolic pathways in plants, but its relationship to PCD is unknown. Here, we show that the shikimate pathway promotes PCD in Arabidopsis. We identify a photoperiod-dependent lesion-mimic mutant named *Lesion in short-day (lis)*, which forms spontaneous lesions in short-day conditions. Map-based cloning and whole-genome resequencing reveal that *LIS* encodes MEE32, a bifunctional enzyme in the shikimate pathway. Metabolic analysis shows that the level of shikimate is dramatically increased in *lis*. Through genetic screenings, three suppressors of *lis* (*slis*) are identified and the causal genes are cloned. *SLISes* encode proteins upstream of MEE32 in the shikimate pathway. Furthermore, exogenous shikimate treatment causes PCD. Our study uncovers a link between the shikimate pathway and PCD, and suggests that the accumulation of shikimate is an alternative explanation for the action of glyphosate, the most successful herbicide.

Copyright © 2022, Institute of Genetics and Developmental Biology, Chinese Academy of Sciences, and Genetics Society of China. Published by Elsevier Limited and Science Press. All rights reserved.

### Introduction

Programmed cell death (PCD) is a genetically regulated process that leads to cell suicide in all multicellular organisms. It occurs during both development (known as dPCD) and the responses to environment (known as ePCD). In plants, dPCD is involved in many processes including xylem formation, embryogenesis, pollen maturation, seed maturation, and leaf senescence (Van Hautegeem et al., 2015). ePCD is very important for plants to defense against environmental stresses including both abiotic stresses (e.g., salt stress, drought stress, cold stress, and heat stress) and biotic stresses (e.g., pathogens and insects). One of the most well-studied forms of ePCD in plants is the hypersensitive response (HR), which occurs upon pathogen infection (Jones and Dangl, 2006). Given the pivotal importance of PCD, its deficiency causes many severe consequences including cancers in animals (Roos et al., 2016). Compared with the mechanisms of animal PCD, the molecular

networks underlying plant PCD are poorly understood (Valandro et al., 2020).

The identifications and characterizations of lesion-mimic mutants (LMMs) greatly help to elucidate the mechanisms of plant PCD (Lorrain, 2003; Bruggeman et al., 2015). LMMs form spontaneous PCD in the absence of pathogen infections. In many cases, the suppressors of LMMs were also identified through genetic screenings. These studies revealed that the chloroplast plays a pivotal role in plant PCD (op den Camp et al., 2003; Yang et al., 2012; Lv et al., 2019; Zhi et al., 2019). In addition, the formation of PCD is closely related to reactive oxygen species (ROS), plant hormones (such as salicylic acid, ethylene, and jasmonic acid), lipids (such as sphingolipids and fatty acids), and calcium signals (Przybyla et al., 2008; Mandal et al., 2012; Landoni et al., 2013; Ma et al., 2016; Radojicic et al., 2018; Bi et al., 2021; Jacob et al., 2021). These signals will eventually regulate the expression of PCD-related genes at the transcriptional level and post-transcriptional levels. One of the most well-studied LMMs is the *Isd1* mutant, in which a zinc finger domain-containing protein (AT4G20380) was mutated (Dietrich et al., 1994). The studies on *Isd1* revealed that metacaspases (MC), the distant homolog of caspase, play important roles in plant PCD (Coll et al., 2010). It was found that the Arabidopsis MC1 and MC2 have

\* Corresponding author.

E-mail address: [spyang@mail.hzau.edu.cn](mailto:spyang@mail.hzau.edu.cn) (S. Yan).

opposite effects in PCD, with MC1 positively regulating PCD and MC2 negatively regulating PCD (Coll et al., 2010). It is expected that the identification of more LMMs will further enhance our understanding of PCD.

The shikimate pathway in the chloroplast is one of the most important metabolic pathways in plants. More than 30% of the carbon fixed by photosynthesis enters the shikimate pathway (Maeda and Dudareva, 2012). The shikimate pathway starts with two substrates, phosphoenolpyruvate (PEP) produced by glycolysis and erythrose-4-phosphate (E4P) produced by the pentose phosphate pathway, and ends with chorismate through a seven-step enzymatic reaction (Fig. S1). Chorismate is not only a common precursor of aromatic amino acids (phenylalanine, tyrosine, and tryptophan), but also a precursor of many secondary metabolites (such as alkaloids and flavonoids). It is noted that chorismate and phenylalanine are the precursors of salicylic acid, the plant immune hormone and important regulator of PCD (Radojicic et al., 2018). Although the role of salicylic acid in PCD has been well-established, it remains unknown whether the shikimate pathway itself regulates PCD.

In this study, we identify an LMM named *lis* (for Lesion in short-day), which formed lesions in short-day conditions, but not in long-day conditions. *LIS* encodes an enzyme involved in the shikimate pathway and the shikimate level was enhanced in the *lis* mutant. Through genetic screening, three suppressors of *lis* (*slis1*, *slis2*, and *slis3*) are identified, and their corresponding causal genes are cloned. *SLISes* encode proteins upstream of MEE32 in the shikimate pathway and their loss of functions reduced the shikimate level. In addition, exogenous shikimate treatment could induce PCD. Our study suggest that the shikimate pathway promotes PCD, providing new insights into plant PCD.

## Results

### The *lis* mutant undergoes spontaneous PCD in short-day condition

The *lis* mutant grew similarly to wildtype (WT) in long-day (LD) condition (16 h light/8 h dark), but it was much smaller and formed visible lesion in short-day (SD) condition (8 h light/16 h dark; Fig. 1A). To further analyze the cell death phenotype, we carried out trypan-

blue staining assays, in which the dead cells could be stained. As shown in Fig. 1B, clear blue sectors could be observed in the leaves of the *lis* mutant grown in SD condition. Previous studies suggested that ROS is one of the causes of cell death in many LMMs (Kaurilind et al., 2015). Therefore, we examined the levels of H<sub>2</sub>O<sub>2</sub> in the leaves by performing 3,3'-diaminobenzidine (DAB) staining. As shown in Fig. 1C, the levels of H<sub>2</sub>O<sub>2</sub> were much higher in the *lis* mutant grown in SD condition than others. These results suggested that the *lis* mutant grown in SD condition accumulates ROS and triggers cell death.

To further examine the roles of photoperiod in promoting cell death in *lis*, we transferred the two-week-old *lis* seedlings grown in LD to SD. The lesion phenotype was observed three days after transferring and became more obvious afterwards (Fig. 1D). Trypan-blue staining revealed that cell death occurred two days after transferring (Fig. 1E). In consistence, the levels of H<sub>2</sub>O<sub>2</sub> also increased two days after transferring (Fig. 1F). Taking advantage of the transferring experiment, we next sought to examine the importance of the light length or dark length in PCD in *lis*. The *lis* mutant was first grown in 16 h of light and 8 h of dark and then it was transferred to a growth chamber with 8 h of dark length but decreasing length of light. As shown in Table S1, the PCD phenotype occurred when the light length was 11 h or less, suggesting that the light length is important for PCD formation. Alternatively, the *lis* mutant was transferred to a growth chamber with 16 h of light but increasing length of dark. In this case, the PCD phenotype occurred when the dark length was 13 h or more, suggesting that the dark length is also important for PCD formation. Since both the dark length and the light length were important, it is possible that the relative length (or the ratio) of light and dark may be the determinant of PCD. A more detailed analysis is required to determine the ratio.

### *LIS* encodes an enzyme involved in the shikimate pathway

To map the *LIS* locus, we first performed map-based cloning (Lukowitz et al., 2000). The *lis* mutant (in Columbia-0 [Col-0] background) was crossed to Landsberg *erecta* (Ler) and the plants with lesion phenotype in the F<sub>2</sub> population were used for mapping. The *LIS* locus was mapped to the region between the markers F2O10 and T22K18 in Chromosome 3 (Fig. 2A). Then, we performed whole-genome resequencing using the next-generation sequencing

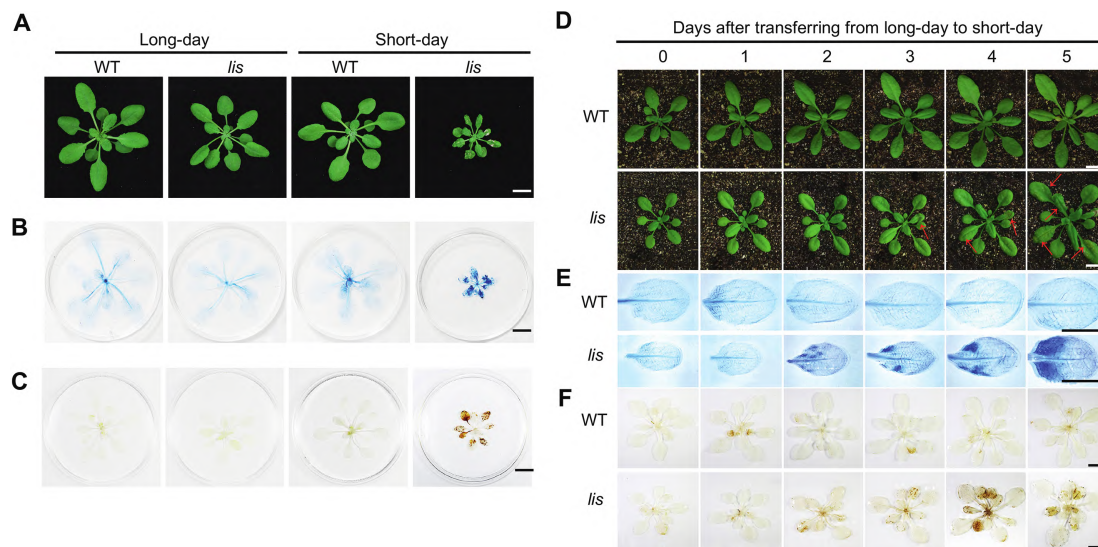


**Fig. 1.** The *lis* mutant is a lesion-mimic mutant in short-day conditions. **A–C:** The phenotypes of wild-type (WT) Arabidopsis and *lis* grown in long-day (LD) or short-day (SD) conditions for three weeks. **D–F:** The phenotypes of WT and *lis* grown in LD conditions for two weeks and then were transferred to SD for different times. **B** and **E:** Trypan blue staining showing the cell death phenotype. **C** and **F:** DAB staining showing the H<sub>2</sub>O<sub>2</sub> levels. The red arrows indicate the leaves undergo cell death. Scale bar, 1 cm.

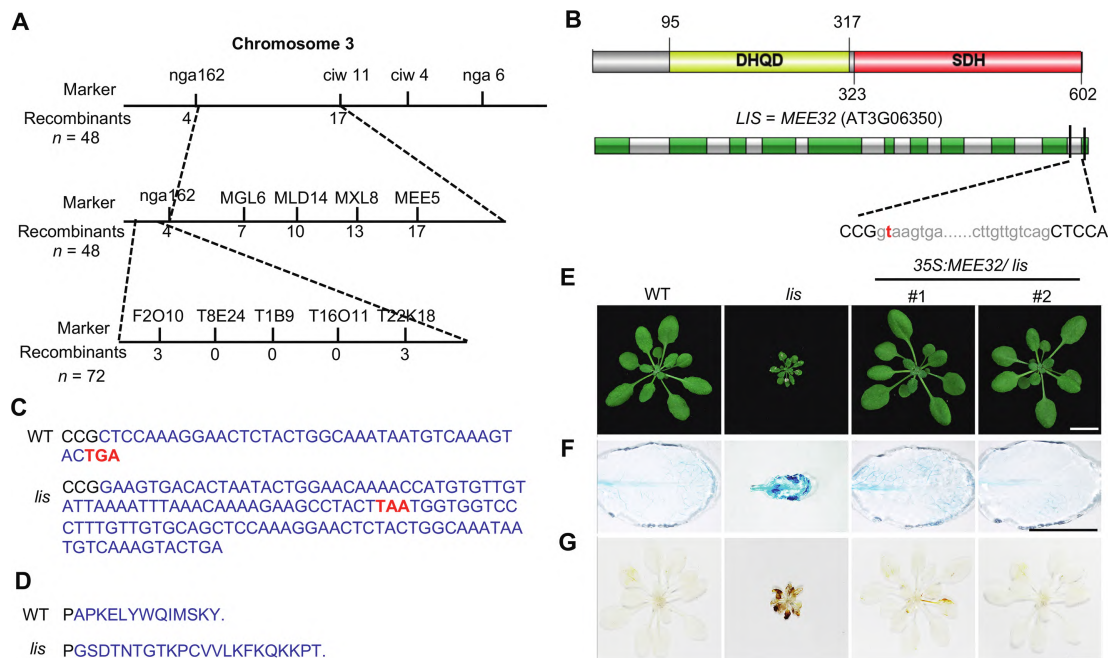


**Fig. 2.** LIS encodes MEE32 involved in the shikimate pathway. **A:** Map-based cloning of LIS. The numbers of recombinants at each marker are shown. **B:** The protein and gene structure of LIS/MEE32. Yellow box indicates DHQD domain. Red box indicates SDH domain. Green boxes indicate exons. Grey boxes indicate introns. In the *lis* mutant, there is a “t” (in red) deletion at the splicing donor site of the last intron. **C:** The 3' cDNA sequence of MEE32 in WT and *lis*. The nucleotides in blue are different. The nucleotides in red are stop codons. **D:** The C-terminal protein sequence of MEE32 in WT and *lis*. The amino acids in blue are different. **E–G:** The phenotypes of WT, *lis*, and the complementation lines (35S:MEE32/*lis*) grown in SD conditions for three weeks. Trypan blue staining showed the cell death phenotype (F). DAB staining showing the  $H_2O_2$  levels (G). SD, short-day. Scale bars, 1 cm.

technology, which helped us to identify two mutated genes (*AT3G06350* and *AT3G07070*) between the two markers. To determine the causal gene, we carried out complementation experiment. The coding sequences (CDSs) of *AT3G06350* or *AT3G07070* driven by the cauliflower mosaic virus 35S promoter were transformed into the *lis* mutant. The resulting transgenic plants expressing *AT3G06350* were similar to WT in SD, suggesting that *AT3G06350* complemented *lis* (Fig. 2E–2G). In *lis*, there was a nucleotide deletion (t) at the conserved splicing donor site of the last intron in *AT3G06350* (Fig. 2B). Therefore, the last intron could not be spliced properly. Indeed, the PCR product of cDNA was larger in *lis* than that in WT (Fig. S2). Sequencing analysis further confirmed that the last intron was retained in *lis* (Fig. 2C). *AT3G06350* was annotated as *embryo defective 3004* (*EMB3004*) or *maternal effect embryo arrest 32* (*MEE32*), which is a bifunctional enzyme with the activities of 3-dehydroquinate dehydratase (DHQD) and shikimate dehydrogenase (SDH) involved in the shikimate pathway (Fig. S1). In the *lis* mutant, the last 13 amino acid residues were replaced (Fig. 2D), which may affect the SDH activity of MEE32.

### The SDH activity of mutated MEE32 is reduced

To confirm the SDH activity was affected in *lis*, we compared the enzymatic activity of MEE32 and the mutated form of MEE32 (MEE32m). The activity of SDH is commonly measured by monitoring the  $NADP^+$ -dependent oxidation of shikimate at 340 nm. The His-SUMO tagged MEE32 or MEE32m proteins were expressed in *E. coli* and were purified through affinity chromatography. The kinetics of MEE32 and MEE32m were illustrated by the Michaelis–Menten curves (Fig. 3A and 3B), which revealed that the  $K_m$  value of MEE32m was similar to that of MEE32, but the  $V_{max}$  value of MEE32m was about 0.4% that of MEE32. Therefore, the SDH activity of MEE32m was indeed dramatically reduced.

Since the activity of MEE32m was reduced, it is likely that the levels of the metabolites related to shikimate change in the *lis* mutant. To test this hypothesis, we determined the contents of these

metabolites through liquid chromatography-mass spectrometry (LC-MS) analysis. Unexpectedly, both the levels of 3-dehydroshikimate (297-fold) and shikimate (24-fold) in *lis* were much higher than those in WT (Fig. 3C). Since salicylic acid is an important regulator of PCD and its biosynthesis is dependent on the shikimate pathway, we also measured the level of salicylic acid. As expected, the salicylic acid level in *lis* was higher than that in WT (Fig. 3C).

### Salicylic acid is not required for PCD of the *lis* mutant

To study the mechanisms underlying the PCD phenotype of *lis*, we performed transcriptome analysis using RNA sequencing (RNA-Seq) to identify the differentially expressed genes after *lis* was transferred from LD to SD for two days. Volcano plot analysis revealed that 2763 genes were significantly up-regulated and 954 genes were significantly down-regulated after transferring ( $P < 0.05$ ,  $|\text{Log}_2\text{FoldChange}| \geq 1$ ; Fig. 4A). Gene ontology (GO) analysis showed that the up-regulated genes are mainly involved in stress responses (Fig. 4B) and the down-regulated genes are mainly related to metabolisms (Fig. S3). In consistence with the PCD phenotype, the genes related to immune response and cell death were significantly enriched (Fig. 4B). Notably, the genes responsive to salicylic acid were also enriched (Fig. 4B). Since salicylic acid is required for PCD of many LMMs (Meng et al., 2009; Huang et al., 2018) and the salicylic acid level was increased in *lis* (Fig. 3C), we hypothesized that blocking salicylic acid biosynthesis or signaling may suppress PCD of *lis*.

In Arabidopsis, ICS1/SID2 is required for salicylic acid biosynthesis (Wildermuth et al., 2001) and NPR1 is required for salicylic acid signaling (Cao et al., 1997). To test our hypothesis, we crossed the *lis* mutant with both the *sid2-1* mutant and the *npr1-1* mutant to generate *lis sid2-1* and *lis npr1-1* double mutants. As shown in Fig. 4C–4H, the plant size, cell death, and ROS levels of the double mutants were similar to *lis* in SD, suggesting that PCD of *lis* is not caused by the increased level of salicylic acid.

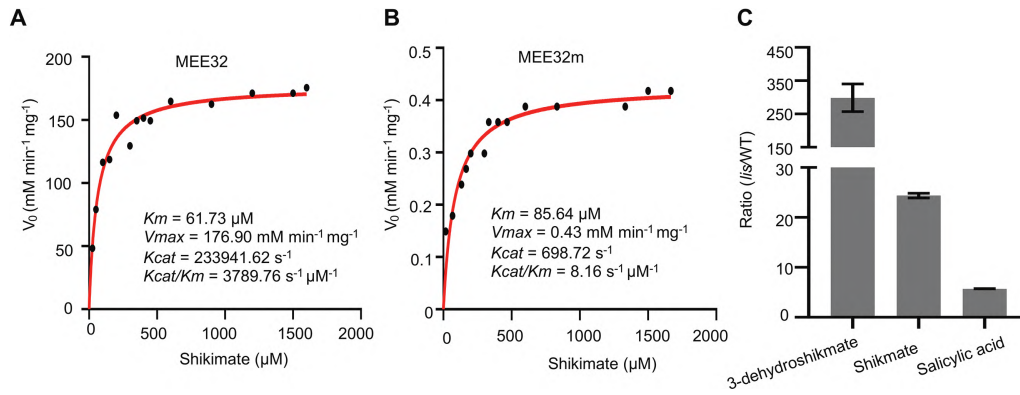


**Fig. 3.** The activity of MEE32m is reduced. **A** and **B**: The enzyme kinetics of MEE32 (**A**) and MEE32m (**B**). The recombinant His-SUMO-MEE32 and His-SUMO-MEE32m were expressed in *E. coli* and purified using Ni-NTA beads. Shikimate was used as substrate. The data were fitted using the Michaelis-Menten model in GraphPad to obtain  $K_m$ ,  $K_{cat}$ , and  $V_{max}$ . **C**: The concentration ratios of 3-dehydroshikimate, shikimate, and salicylic acid in *lis* relative to WT.

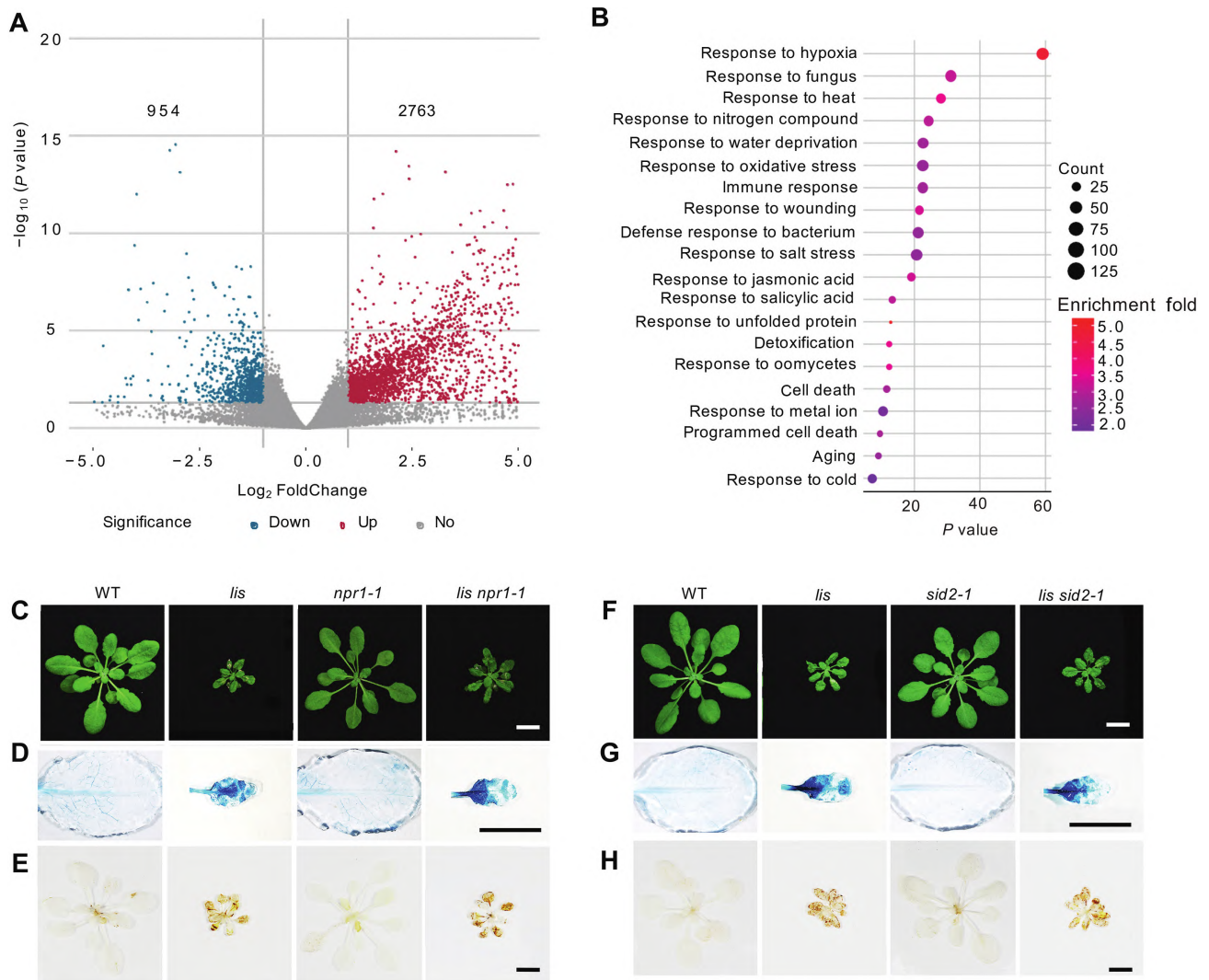


**Fig. 4.** The phenotype of *lis* is independent of salicylic acid. **A**: Volcano plots showing the differentially expressed genes after *lis* were transferred from LD to SD for two days ( $P < 0.05$ ,  $|\text{Log}_2\text{FoldChange}| \geq 1$ ). The red dots represent significantly up-regulated genes, and the blue dots represent significantly down-regulated genes. **B**: Gene ontology enrichment analysis of the up-regulated genes. The size of each dot represents the gene count, and the color of each dot represents the enrichment fold. **C–H**: The phenotypes of WT, *lis*, *npr1-1*, *sid2-1*, *lis npr1-1*, and *lis sid2-1* grown in SD condition for three weeks. **D** and **G**: Trypan blue staining showing the cell death phenotype. **E** and **H**: DAB staining showing the  $\text{H}_2\text{O}_2$  levels. LD, long-day; SD, short-day. Scale bar, 1 cm.



cells and dead cells, respectively. Consistently, the dead cells increased with the concentration of shikimate used (Fig. 6B).

Next, we sought to test whether overexpression of *MEE32m* in WT could induce cell death. We could not obtain transgenic lines expressing *MEE32m* driven by the 35S promoter, indicating that overexpression of *MEE32m* triggers cell death, leading to embryonic lethality. To solve this problem, we used a dexamethasone (DEX)-inducible promoter to drive the expression of *MEE32m-GFP*. The transgenic plants grew normally without DEX treatment. However, after DEX treatment, the transgenic plants became smaller and developed lesions in leaves (Fig. 6C). The induced expression of *MEE32m-GFP* was confirmed through western blotting analysis (Fig. S5). These results suggested that the enhanced level of shikimate is sufficient to trigger cell death.

## Discussion

LMMs played key roles in elucidating the mechanism of PCD (Eremina et al., 2015). In this study, we identified a photoperiod-dependent LMM, *lis*, which underwent PCD only in SD conditions (Fig. 1). The identification of *lis* provided us with a new opportunity to study the mechanism of PCD. In the *lis* mutant, the levels of both 3-dehydroshikimate and shikimate, were dramatically elevated (Fig. 3). In addition, mutations in proteins upstream of LIS in the shikimate pathway suppressed PCD of *lis* (Fig. 5). These data suggested that the enhanced shikimate pathway promotes PCD, thereby uncovering a link between the shikimate pathway and PCD. However, the biological significance of this link remains to be further studied. It is expected that the shikimate pathway may function in stress responses.

Our study suggested that in addition to as an important metabolic intermediate, shikimate can also function as a signaling molecule. Previously, several metabolites including sugars and amino acids

were found to function as signals to regulate fundamental biological processes (Templeton and Moorhead, 2004). And the glucose sensing and signaling pathways have been well-studied in plants, with HXK1 as the glucose sensor and VHA-B1 and RPT5B as transcriptional regulators (Cho et al., 2006). Recently, it was found that malate is also a regulator of cell death in Arabidopsis (Zhao et al., 2018). More interestingly, they showed that malate treatment could induce cell death even in animal cells. It will be interesting to test whether shikimate can also trigger cell death in animal cells in the future. When applied exogenously, only high concentration of shikimate (40 mM for Arabidopsis and 10 mM for BY2 cells) can induce cell death (Fig. 6A and 6B). This could be because exogenously applied shikimate is difficult to enter cells. Alternatively, this may be a common feature when metabolites function as signals. In the case of glucose signaling, 5% (>250 mM) of glucose was used to treat plants (Cho et al., 2006). In the case of malate, 50 mM was shown to induce cell death (Zhao et al., 2018). It is of note that although shikimate treatment induces PCD, we cannot rule out the possibility that 3-dehydroquinate and the metabolites downstream of shikimate such as aromatic amino acids can also contribute to PCD in *lis*.

As one of the most important metabolic pathways, the shikimate pathway is essential for plants (Gout et al., 1992; Maeda and Dudareva, 2012). Therefore, it is difficult to study the relationship between the shikimate pathway and PCD based on loss-of-function mutants. In this study, we obtained a unique *lis* mutant, in which the mutant *MEE32* showed reduced enzyme activity but the levels of 3-dehydroshikimate and shikimate increased (Fig. 3). It is possible that there is a feedback regulation mechanism of the shikimate pathway. The reduced flow from 3-dehydroshikimate to shikimate may enhance the carbon flow into the shikimate pathway, thereby increasing the level of 3-dehydroshikimate, which was 297-fold in the *lis* mutant compared with WT (Fig. 3C). The 3-dehydroshikimate were

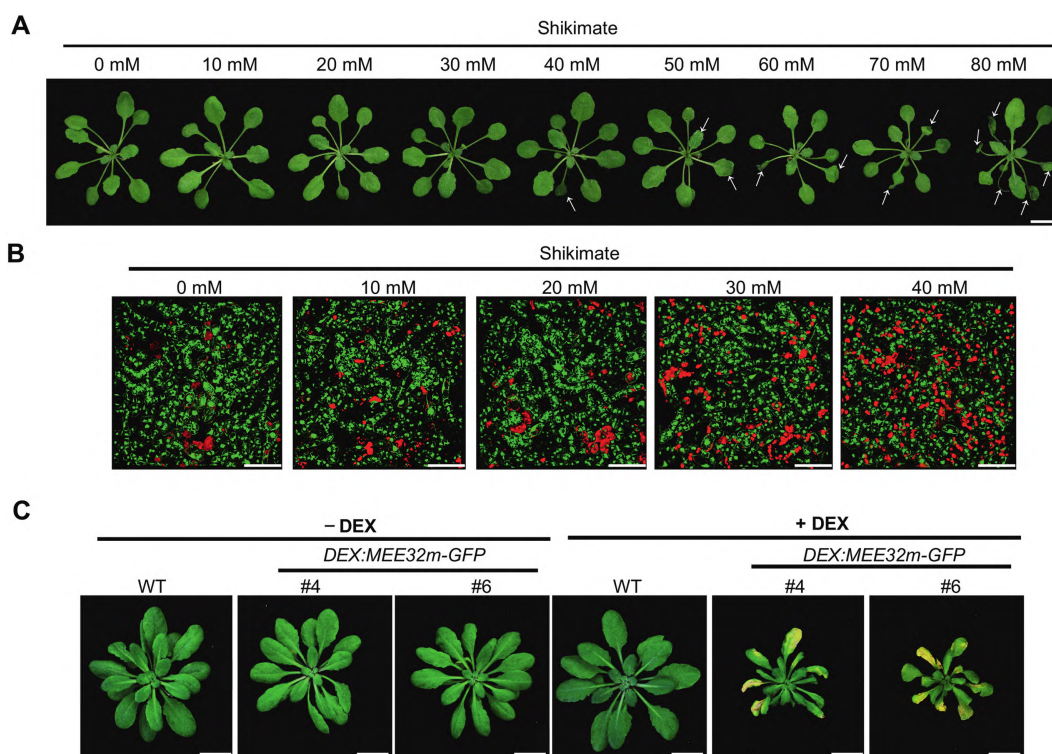


**Fig. 6.** Shikimate induces cell death. **A:** The phenotypes of WT Arabidopsis treated with different concentrations (pH 7.0) of shikimate for three days. The white arrows indicate the leaves undergo cell death. **B:** The FDA/PI staining results of tobacco BY2 suspension cells treated with different concentrations of shikimate (pH 5.7) for 24 h. Green signals indicate live cells and red signals indicate dead cells. **C:** The phenotypes of WT and the transgenic Arabidopsis expressing *MEE32m-GFP* driven by the dexamethasone (DEX)-inducible promoter. The plants were treated with (+) or without (-) 25  $\mu$ M DEX for 10 days. Scale bars, 1 cm (**A** and **C**); 250  $\mu$ m (**B**).

slowly catalyzed into shikimate eventually. Alternatively, it is also possible that the mutation in *lis* may enhance the activity of DHQD, thereby enhancing the level of 3-dehydroshikimate, which is catalyzed into shikimate. It is of note that the heterozygous plants (*LIS*<sup>-/+</sup>) displayed WT phenotypes, suggesting that *lis* was a recessive mutant.

Our results also provided an alternative explanation for the action of glyphosate, the most successful herbicide in history (Benbrook, 2016). It is well-known that glyphosate specifically inhibits the activity of the enzyme 5-enolpyruvylshikimate-3-phosphate synthase (EPSPS), one of the key enzymes in the shikimate pathway (Steinrücken and Amrhein, 1980). However, it remains debatable how glyphosate kills plants. Currently, there are two popular hypotheses. One hypothesis suggested that the inhibition of EPSPS by glyphosate results in insufficient production of aromatic amino acids, which are vital for protein synthesis and plant growth (Schonbrunn et al., 2001). The other hypothesis argued that glyphosate enhanced the carbon flow into the shikimate pathway, which results in the shortages of carbon for other essential pathways (Duke and Powles, 2008). It was reported that glyphosate-treated plant tissues accumulated high levels of shikimate (Schulz et al., 1990; Zulet-Gonzalez et al., 2020). The concentration of shikimate in cellular compartments excluding the vacuole was estimated to be 100 mM–150 mM (Gout et al., 1992). In our study, we found that the level of shikimate in *lis* was 24-fold of WT (Fig. 3C) and exogenous shikimate treatment could induce cell death (Fig. 6A and 6B). Therefore, the glyphosate-triggered shikimate accumulation may be an alternative reason for glyphosate in killing plants.

## Materials and methods

### Plant materials and growth conditions

All *Arabidopsis* mutants used in this study were in Col-0 background. The *npr1-1* and *sid2-1* mutants were described previously (Cao et al., 1997; Wildermuth et al., 2001). Seeds were sterilized with 2% plant preservation mixture (plant cell technology) and stratified at 4°C in the darkness for two days. The plants were grown in different day length (light intensity is 100 μmol photons m<sup>-2</sup> s<sup>-1</sup>; supplied by white-light tubes) at 22°C. The primers used for genotyping were listed in Table S5.

### Suppressor screening

The *lis* seeds were mutagenized with 0.2% ethylmethanesulfonate (EMS). The M1 plants were grown in soil to produce M2 seeds, which were collected from individual M1 plants. To screen for suppressors of *lis*, the M2 seeds were grown in SD conditions in soils. The plants without lesions on leaves were considered to be the suppressors.

### Map-based cloning and whole-genome resequencing

To clone *LIS* and *SLIS1*, we performed map-based cloning. The mutants (in Col-0 background) were crossed with *Ler*. To clone *LIS*, the plants with lesions in the F2 population were selected for mapping and resequencing. To clone *SLIS1*, the plants without lesions but in *lis* background were selected for mapping. The mapping was carried out according to a previous study (Lukowitz et al., 2000) and additional markers were designed at *Arabidopsis* mapping platform (<http://amp.genomics.org.cn/>). To clone *SLIS2* and *SLIS3*, the *lis slis2* and *lis slis3* mutants were crossed with *lis* and the plants without lesion phenotype in the F2 population were selected for resequencing. The resequencing was performed by Novogene (Beijing, China). The SIMPLE pipeline (Wachsman et al., 2017) was used to analyze the data to obtain candidate genes.

## Construction of plasmids

The vectors were constructed using digestion–ligation method, lighting cloning system (BDIT0014, Biodragon Immunotechnology), or Gateway technology (Thermo Fisher). The coding sequences of genes were used for vector construction. For complementation test, *MEE32* was cloned into *pEarlyGate 100* using Gateway technology; *DHS1*, *PPT1*, and *ENO2* were cloned into *Nco I/Xba I*-digested *pFGC5941*. To generate *DEX:MEE32m-GFP*, *MEE32m* were fused with linker sequence (CCAGGCGGCGGCGGCTCCGCGGCGGCCCA) and *GFP* by fusion PCR, and was then cloned into *Spe I/Xho I*-digested *pTA7002*. For protein expression in *E. coli*, *MEE32* and *MEE32m* were cloned into *BamH I/Xho I*-digested *pEF28b-SUMO* to generate *His-SUMO-MEE32* or *His-SUMO-MEE32m*. The primers used for cloning were listed in Table S5.

## Trypan blue staining

Trypan blue staining was performed as previously described with minor modifications (Yan et al., 2013). In brief, plants were immersed with trypan blue staining solution (10 mL phenol, 10 mL H<sub>2</sub>O, 10 mL glycerol, 10 mL lactic acid, and 25 mg trypan blue), boiled for 2–3 min, and then cooled down at room temperature for 1 h. The samples were destained in 2.5 g/mL chloral hydrate solution.

## DAB staining

H<sub>2</sub>O<sub>2</sub> was detected as previously described (Thordal-Christensen et al., 1997). Briefly, plants were immersed in DAB staining solution (1 mg/mL DAB, pH 3.8) and vacuumed for 10 min. DAB staining was carried out in a 28°C incubator for 6–8 h. After staining, plants were destained in acetic acid: glycerol:ethanol (1:1:3, v/v/v) solution at 100°C for 10 min, and were then stored in 95% (v/v) ethanol until scanning.

## Measurement of the content of metabolites in the shikimate pathway

Sample preparation and quantification were as described previously (Chen et al., 2013). The leaves were frozen in liquid nitrogen and were crushed using a mixer mill (MM 400, Retsch) with a zirconia bead for 1.5 min at 30 Hz. About 100 mg powder was weighed and extracted overnight at 4°C with 1 mL 70% aqueous methanol containing 0.1 mg L<sup>-1</sup> lidocaine (internal standard) before analysis using an LC-ESI-MS/MS system.

## Enzyme kinetics analysis

The SDH activity was measured as described previously (Singh and Christendat, 2006). Briefly, the His-SUMO tagged *MEE32* and *MEE32m* proteins were added into reaction mixtures containing different concentrations of shikimate, 100 mM Tris-HCl, pH 8.8, and 2 mM NADP<sup>+</sup> (N196976, Aladdin). The enzymatic activity was determined by monitoring the reduction of NADP<sup>+</sup> at 340 nm in the presence of shikimate. The data were analyzed using GraphPad.

## Measurement of shikimate content

The shikimate content was determined as described previously (Shaner et al., 2005). The leaf discs were incubated in 1 mL 10 mM ammonium phosphate (pH 4.4). The samples were frozen at –20°C freezer and then were thawed at 60°C for 30 min. After adding 0.25 mL 1.25 M HCl, the samples were further incubated at 60°C for 15 min to extract metabolites. The resulting supernatant (0.25 mL) was mixed with 1 mL 0.25% (w/v) periodic acid and incubated at

room temperature for 90 min. The reaction was stopped by adding 1 mL 0.6 M sodium hydroxide. The absorption at 380 nm was measured. The shikimate concentration was determined based on a standard curve.

### Western blotting analysis

The total proteins were extracted using extraction buffer (20 mM Tris-HCl pH 7.5, 150 mM NaCl, 1% Triton X-100, 1× protease inhibitor cocktail, and 1 mM PMSF (BL507A, Biosharp) and were subjected to western blotting using an anti-GFP (1:4000, Promoter) antibody.

### Transcriptome analysis

Total RNA was extracted with TRizol reagent (Invitrogen) from 2-week-old *lis* after *lis* was transferred from LD to SD for two days. Library preparation and RNA-sequencing were performed by Novogene (Beijing, China). Raw reads were processed and aligned to the Arabidopsis genome (<https://www.arabidopsis.org>) using Hisat2, version 2.5.1b. The transcript assembly and read quantification were performed by StringTie (Kim et al., 2019). Genes with over 20 reads were filtered and processed using DESeq2 to identify the differentially expressed genes ( $P < 0.05$ ,  $|\text{Log}_2\text{FoldChange}| \geq 1$ ). GO analysis was carried out using PANTHER Classification System database (<http://pantherdb.org/>).

### Shikimate treatment

Two-week-old WT grown in LD condition were sprayed with different concentrations of shikimate (S107142, Aladdin) after being transferred to SD condition. Shikimate (adjusted to pH 7.0) treatment was carried out once per day for three days. BY2 cells were cultured in MS medium with 0.4  $\mu\text{g}/\text{mL}$  2,4-D, 1  $\mu\text{g}/\text{mL}$  thiamine, and 100  $\mu\text{g}/\text{mL}$  Myo-inositol, followed by treatment with different concentrations of shikimate (adjusted to pH 5.7) for 24 h. FDA/PI staining was performed as previously described (Jones et al., 2016). The fluorescence of FDA and PI was captured using a confocal microscopy (Leica SP8).

### Data availability

The RNA-seq data and the whole-genome sequencing data generated in this study have been deposited in BioProject database (PRJNA767202).

### CRedit authorship contribution statement

**Xuerui Lu:** Conceptualization, Data curation, Methodology, Formal analysis, Investigation, Validation, Writing - Original draft, Writing - Review & Editing. **Shishi Xi:** Data curation, Investigation, Validation. **Chong Wu:** Formal analysis, Software. **Xueao Zheng:** Formal analysis, Software. **Chenkun Yang:** Data curation, Methodology. **Jie Luo:** Conceptualization, Project administration, Resources. **Shunping Yan:** Conceptualization, Resources, Funding acquisition, Supervision, Project administration, Writing - Review & Editing.

### Conflict of interest

The authors declare that they have no conflict of interest.

### Acknowledgments

We thank Dr. Ting Pan for the helpful discussion and Dr. Lianhuan Qu for the help in metabolic analysis. This work was supported

by grants from the National Natural Science Foundation of China (31771355 and 31970311), Thousand Talents Plan of China-Young Professionals, and Huazhong Agricultural University Scientific & Technological Self-innovation Foundation (2014RC004).

### Supplementary data

Supplementary data to this article can be found online at <https://doi.org/10.1016/j.jgg.2022.02.001>.

### References

- Abe, A., Kosugi, S., Yoshida, K., Natsume, S., Takagi, H., Kanzaki, H., Matsumura, H., Yoshida, K., Mitsuoka, C., Tamiru, M., et al., 2012. Genome sequencing reveals agronomically important loci in rice using mutmap. *Nat. Biotechnol.* 30, 174–178.
- Benbrook, C.M., 2016. Trends in glyphosate herbicide use in the United States and globally. *Environ. Sci. Eur.* 28, 3.
- Bi, G., Su, M., Li, N., Liang, Y., Dang, S., Xu, J., Hu, M., Wang, J., Zou, M., Deng, Y., et al., 2021. The ZAR1 resistosome is a calcium-permeable channel triggering plant immune signaling. *Cell* 184, 3528–3541.
- Bruggeman, Q., Raynaud, C., Benhamed, M., Delarue, M., 2015. To die or not to die? Lessons from lesion mimic mutants. *Front. Plant Sci.* 6, 24.
- Cao, H., Glazebrook, J., Clarke, J.D., Volko, S., Dong, X., 1997. The Arabidopsis *NPR1* gene that controls systemic acquired resistance encodes a novel protein containing ankyrin repeats. *Cell* 88, 57–63.
- Chen, W., Gong, L., Guo, Z., Wang, W., Zhang, H., Liu, X., Yu, S., Xiong, L., Luo, J., 2013. A novel integrated method for large-scale detection, identification, and quantification of widely targeted metabolites: application in the study of rice metabolomics. *Mol. Plant* 6, 1769–1780.
- Cho, Y.H., Yoo, S.D., Sheen, J., 2006. Regulatory functions of nuclear hexokinase1 complex in glucose signaling. *Cell* 127, 579–589.
- Coll, N.S., Vercammen, D., Smidler, A., Clover, C., Van Breusegem, F., Dangl, J.L., Epple, P., 2010. Arabidopsis type I metacaspases control cell death. *Science* 330, 1393–1397.
- Dietrich, R.A., Delaney, T.P., Uknes, S.J., Ward, E.R., Ryals, J.A., Dangl, J.L., 1994. Arabidopsis mutants simulating disease resistance response. *Cell* 77, 565–577.
- Duke, S.O., Powles, S.B., 2008. Glyphosate: a once-in-a-century herbicide. *Pest Manag. Sci.* 64, 319–325.
- Eremina, M., Rozhon, W., Yang, S., Poppenberger, B., 2015. ENO2 activity is required for the development and reproductive success of plants, and is feedback-repressed by AtMBP-1. *Plant J.* 81, 895–906.
- Gout, E., Bigny, R., Genix, P., Tissot, M., Douce, R., 1992. Effect of glyphosate on plant cell metabolism.  $^{31}\text{P}$  and  $^{13}\text{C}$  NMR studies. *Biochimie* 74, 875–882.
- Huang, X.X., Zhu, G.Q., Liu, Q., Chen, L., Li, Y.J., Hou, B.K., 2018. Modulation of plant salicylic acid-associated immune responses via glycosylation of dihydroxybenzoic acids. *Plant Physiol.* 176, 3103–3119.
- Jacob, P., Kim, N.H., Wu, F., El-Kasbi, F., Chi, Y., Walton, W.G., Furzer, O.J., Lietzan, A.D., Sunil, S., Kempthorn, K., et al., 2021. Plant “helper” immune receptors are  $\text{Ca}^{2+}$ -permeable nonselective cation channels. *Science* 373, 420–425.
- Jones, J.D., Dangl, J.L., 2006. The plant immune system. *Nature* 444, 323–329.
- Jones, K., Kim, D.W., Park, J.S., Khang, C.H., 2016. Live-cell fluorescence imaging to investigate the dynamics of plant cell death during infection by the rice blast fungus *magnaporthe oryzae*. *BMC Plant Biol.* 16, 69.
- Kaurilind, E., Xu, E., Brosche, M., 2015. A genetic framework for  $\text{H}_2\text{O}_2$  induced cell death in *Arabidopsis thaliana*. *BMC Genom.* 16, 837.
- Kim, D., Paggi, J.M., Park, C., Bennett, C., Salzberg, S.L., 2019. Graph-based genome alignment and genotyping with HISAT2 and HISAT-genotype. *Nat. Biotechnol.* 37, 907–915.
- Knappe, S., Lottgert, T., Schneider, A., Voll, L., Flugge, U.I., Fischer, K., 2003. Characterization of two functional *phosphoenolpyruvate/phosphate translocator (PPT)* genes in *Arabidopsis*—*AtPPT1* may be involved in the provision of signals for correct mesophyll development. *Plant J.* 36, 411–420.
- Landoni, M., De Francesco, A., Bellatti, S., Delle Donne, M., Ferrarini, A., Venturini, L., Pilu, R., Bononi, M., Tonelli, C., 2013. A mutation in the *FZL* gene of *Arabidopsis* causing alteration in chloroplast morphology results in a lesion mimic phenotype. *J. Exp. Bot.* 64, 4313–4328.
- Lorrain, S., 2003. Lesion mimic mutants: keys for deciphering cell death and defense pathways in plants? *Trends Plant Sci.* 8, 263–271.
- Lukowitz, W., Gillmor, C.S., Scheible, W.R., 2000. Positional cloning in Arabidopsis. Why it feels good to have a genome initiative working for you. *Plant Physiol.* 123, 795–805.
- Lv, R., Li, Z., Li, M., Dogra, V., Lv, S., Liu, R., Lee, K.P., Kim, C., 2019. Uncoupled expression of nuclear and plastid photosynthesis-associated genes contributes to cell death in a lesion mimic mutant. *Plant Cell* 31, 210–230.
- Ma, L., Tian, T., Lin, R., Deng, X.W., Wang, H., Li, G., 2016. Arabidopsis *FHY3* and *FAR1* regulate light-induced *myo*-inositol biosynthesis and oxidative stress responses by transcriptional activation of *MIPS1*. *Mol. Plant* 9, 541–557.
- Maeda, H., Dudareva, N., 2012. The shikimate pathway and aromatic amino acid biosynthesis in plants. *Annu. Rev. Plant Biol.* 63, 73–105.

- Mandal, M.K., Chandra-Shekara, A.C., Jeong, R.D., Yu, K., Zhu, S., Chanda, B., Navarre, D., Kachroo, A., Kachroo, P., 2012. Oleic acid-dependent modulation of NITRIC OXIDE ASSOCIATED1 protein levels regulates nitric oxide-mediated defense signaling in *Arabidopsis*. *Plant Cell* 24, 1654–1674.
- Meng, P.H., Raynaud, C., Tcherkez, G., Blanchet, S., Massoud, K., Domenichini, S., Henry, Y., Soubigou-Taconnat, L., Lelarge-Trouverie, C., Saindrenan, P., et al., 2009. Crosstalks between myo-inositol metabolism, programmed cell death and basal immunity in *Arabidopsis*. *PLoS ONE* 4, e7364.
- op den Camp, R.G., Przybyla, D., Ochsenbein, C., Laloi, C., Kim, C., Danon, A., Wagner, D., Hideg, E., Gobel, C., Feussner, I., et al., 2003. Rapid induction of distinct stress responses after the release of singlet oxygen in *Arabidopsis*. *Plant Cell* 15, 2320–2332.
- Prabhakar, V., Lottgert, T., Gigolashvili, T., Bell, K., Flugge, U.I., Hausler, R.E., 2009. Molecular and functional characterization of the plastid-localized phosphoenolpyruvate enolase (ENO1) from *Arabidopsis thaliana*. *FEBS Lett.* 583, 983–991.
- Przybyla, D., Gobel, C., Imboden, A., Hamberg, M., Feussner, I., Apel, K., 2008. Enzymatic, but not non-enzymatic,  $^1\text{O}_2$ -mediated peroxidation of polyunsaturated fatty acids forms part of the EXECUTER1-dependent stress response program in the *flu* mutant of *Arabidopsis thaliana*. *Plant J.* 54, 236–248.
- Radojicic, A., Li, X., Zhang, Y., 2018. Salicylic acid: a double-edged sword for programmed cell death in plants. *Front. Plant Sci.* 9, 1133.
- Roos, W.P., Thomas, A.D., Kaina, B., 2016. DNA damage and the balance between survival and death in cancer biology. *Nat. Rev. Cancer* 16, 20–33.
- Schonbrunn, E., Eschenburg, S., Shuttleworth, W.A., Schloss, J.V., Amrhein, N., Evans, J.N., Kabsch, W., 2001. Interaction of the herbicide glyphosate with its target enzyme 5-enolpyruvylshikimate 3-phosphate synthase in atomic detail. *Proc. Natl. Acad. Sci. U. S. A.* 98, 1376–1380.
- Schulz, A., Münder, T., Holländer-Czytko, H., Amrhein, N., 1990. Glyphosate transport and early effects on shikimate metabolism and its compartmentation in sink leaves of tomato and spinach plants. *Z. Naturforsch. C Biosci.* 45, 529–534.
- Shaner, D.L., Nadler-Hassar, T., Henry, W.B., Koger, C.H., 2005. A rapid in vivo shikimate accumulation assay with excised leaf discs. *Weed Sci.* 53, 769–774.
- Singh, S.A., Christendat, D., 2006. Structure of *Arabidopsis* dehydroquinate dehydratase-shikimate dehydrogenase and implications for metabolic channeling in the shikimate pathway. *Biochemistry* 45, 7787–7796.
- Steinrücken, H.C., Amrhein, N., 1980. The herbicide glyphosate is a potent inhibitor of 5-enolpyruvylshikimate acid-3-phosphate synthase. *Biochem. Biophys. Res. Commun.* 94, 1207–1212.
- Templeton, G.W., Moorhead, G.B., 2004. A renaissance of metabolite sensing and signaling: from modular domains to riboswitches. *Plant Cell* 16, 2252–2257.
- Thordal-Christensen, H., Zhang, Z., Wei, Y., Collinge, D.B., 1997. Subcellular localization of  $\text{H}_2\text{O}_2$  in plants.  $\text{H}_2\text{O}_2$  accumulation in papillae and hypersensitive response during the barley-powdery mildew interaction. *Plant J.* 11, 1187–1194.
- Valandro, F., Menguer, P.K., Cabreira-Cagliari, C., Margis-Pinheiro, M., Cagliari, A., 2020. Programmed cell death (PCD) control in plants: new insights from the *Arabidopsis thaliana* deathosome. *Plant Sci.* 299, 110603.
- Van Hautegeem, T., Waters, A.J., Goodrich, J., Nowack, M.K., 2015. Only in dying, life: programmed cell death during plant development. *Trends Plant Sci.* 20, 102–113.
- Wachsman, G., Modliszewski, J.L., Valdes, M., Benfey, P.N., 2017. A simple pipeline for mapping point mutations. *Plant Physiol.* 174, 1307–1313.
- Wildermuth, M.C., Dewdney, J., Wu, G., Ausubel, F.M., 2001. Isochorismate synthase is required to synthesize salicylic acid for plant defence. *Nature* 414, 562–565.
- Yan, S., Wang, W., Marques, J., Mohan, R., Saleh, A., Durrant, W.E., Song, J., Dong, X., 2013. Salicylic acid activates DNA damage responses to potentiate plant immunity. *Mol. Cell* 52, 602–610.
- Yang, Y., Jin, H., Chen, Y., Lin, W., Wang, C., Chen, Z., Han, N., Bian, H., Zhu, M., Wang, J., 2012. A chloroplast envelope membrane protein containing a putative LrgB domain related to the control of bacterial death and lysis is required for chloroplast development in *Arabidopsis thaliana*. *New Phytol.* 193, 81–95.
- Zhao, Y., Luo, L., Xu, J., Xin, P., Guo, H., Wu, J., Bai, L., Wang, G., Chu, J., Zuo, J., et al., 2018. Malate transported from chloroplast to mitochondrion triggers production of ROS and PCD in *Arabidopsis thaliana*. *Cell Res.* 28, 448–461.
- Zhi, T., Zhou, Z., Qiu, B., Zhu, Q., Xiong, X., Ren, C., 2019. Loss of fumarylacetoacetate hydrolase causes light-dependent increases in protochlorophyllide and cell death in *Arabidopsis*. *Plant J.* 98, 622–638.
- Zulet-Gonzalez, A., Barco-Antonanzas, M., Gil-Monreal, M., Royuela, M., Zabalza, A., 2020. Increased glyphosate-induced gene expression in the shikimate pathway is abolished in the presence of aromatic amino acids and mimicked by shikimate. *Front. Plant Sci.* 11, 459.